

Stability of hypothetical $\text{Ag}^{\text{II}}\text{Cl}_2$ polymorphs under high pressure, revisited – a computational study

Adam Grzelak^{1*} and Wojciech Grochala¹

¹*Center for New Technologies, University of Warsaw, Banacha 2C, 02-097 Warszawa, Poland*

**a.grzelak@cent.uw.edu.pl*

Abstract

A comparative computational study of stability of candidate structures for an as-yet unknown silver dichloride AgCl_2 is presented. It is found that all considered candidates have a negative enthalpy of formation, but are unstable towards charge transfer and decomposition into silver(I) chloride and chlorine within the DFT and hybrid-DFT approaches in the entire studied pressure range. Within SCAN approach, several of the “true” $\text{Ag}^{\text{II}}\text{Cl}_2$ polymorphs (i.e. containing $\text{Ag}(\text{II})$ species) exhibit a region of stability below ca. 20 GPa. However, their stability with respect to aforementioned decomposition decreases with pressure by account of all three DFT methods, which suggests a limited possibility of high-pressure synthesis of AgCl_2 . Some common patterns in pressure-induced structural transitions observed in the studied systems also emerge, which further testify to an instability of hypothetical AgCl_2 towards charge transfer and phase separation.

Introduction

Chemistry of silver(II) compounds constitutes a topic of studies that is both demanding – particularly due to the extremely strong oxidizing properties of these compounds – as well as interesting, as evidenced by the body of works discussing them in relation to oxocuprates – a well-known family of precursors for high-pressure superconductors. [1,2] Inspired by experimental works exploring high-pressure phase transitions of AgF_2 , [3,4] as well as most recent computational study of thermodynamic stability of hypothetical mixed-valence silver fluorides (including at elevated pressure conditions), [5] this work is a continuation to a previous systematic study, which explored relative stability of multiple hypothetical polymorphs of $\text{Ag}^{\text{II}}\text{Cl}_2$ – an as-yet unknown analogue of AgF_2 . [6] The aforementioned study found that a true silver(II) chloride is likely to be unstable towards charge transfer and phase separation into AgCl and Cl_2 at ambient pressure conditions. This work aims to extend these considerations into high-pressure regime, in the hope that applying extreme conditions could stabilize $\text{Ag}^{\text{II}}\text{Cl}_2$. In particular, the previous study found that a layered, AgF_2 -type polymorph of AgCl_2 could be stabilized at a pressure of ca. 35 GPa, due to relatively low molar volume. [6]

The interest in this particular compound stems from its potential similarity to AgF_2 , which has recently been shown to be an excellent analog of oxocuprates in terms of structure and very strong magnetic interactions. [2] In fact, $\text{Ag}^{\text{II}}\text{Cl}_2$ – if obtained, and providing a suitable structural arrangement – could be expected to host even stronger antiferromagnetic superexchange than AgF_2 , due to stronger covalence of $\text{Ag}-\text{Cl}$ bonding, as predicted from differences in electronegativity (Ag : 1.93, Cl : 3.16, F : 3.98 – Pauling scale). Overall, this work is part of a joint computational and experimental effort: to synthesize $\text{Ag}^{\text{II}}\text{Cl}_2$ utilizing high pressure and high temperature experimental techniques, coupled with computational methods providing insight into understanding the expected products and phases. On top of that, the added value of studies in high-pressure regime is that the observed changes in structure and bonding induced by pressure can provide meaningful insight into the chemical nature of the studied compounds. [7]

Results

Stability of AgCl₂ phases

Seven different candidate structures for polymorphs of AgCl₂ were considered in this work. Six of them were derived from the previous, ambient-pressure study. [6] They were:

- AgF₂ type – corrugated layers made up of [AgCl₄] square subunits;
- CuCl₂ type – 1D chains made up of [AgCl₄] square subunits;
- AuCl₂ type – a kind of nanotubular polymorph derived from OD molecular structure of AuCl₂ (see below);
- Ag(I)r type – a structure composed of double layers of rocksalt-type AgCl interspersed with Cl₂ bridges;
- Ag(I)h type – similar as above, but with hexagonal double layers of AgCl;
- MnO₂ type – a different arrangement of corrugated layers made up of pairs of [AgCl₄] square subunits.

Additionally, the high-pressure, nanotubular polymorph of AgF₂ (referred to as AgF₂ HP) was considered as a candidate. [4] Structures of selected polymorphs described above are presented in fig. 1.

Importantly, Ag(I)r and Ag(I)h polymorphs do not contain Ag(II) species and instead are composed of sub-structures of Ag^ICl and Cl₂ molecules. For the remaining five Ag^{II}Cl₂ polymorphs containing paramagnetic d⁹ silver cation, magnetic interactions were taken into account:

- AgF₂ type: 2D antiferromagnetic (AFM) coupling within layers;
- CuCl₂ type: AABB-type AFM coupling within chains, known to exist in CuCl₂, [8] and found to be the lowest-energy magnetic solution for AgCl₂ in this arrangement; [6]
- AgF₂ HP type: magnetic dimers coupled along ~180 degrees Ag-F-Ag bridges within nanotubes;
- MnO₂ type: AABB-type AFM coupling – ferromagnetic (FM) between adjacent [AgCl₄] squares and AFM between pairs.

The AuCl₂ type derives from a structure of gold(I,III) chloride, a mixed-valence compound which consists of Au₄Cl₈ molecules, each containing two Ag(I) and two Ag(III) species. [9] When this structure is taken as a starting point for geometry optimization, all three computational methods yield a nanotubular polymorph somewhat similar to the AgF₂ HP type. However, only the HSE06 approach is able to reproduce the mixed-valence nature of AuCl₂ and of the corresponding nanotubular polymorph of AgCl₂ derived from the former (as evidenced by two different coordination patterns of Ag sites in that solution). [6] On the other hand, in the PBEsol+U and SCAN calculations, a magnetic model with dimers as in the AgF₂ HP type polymorphs was considered.

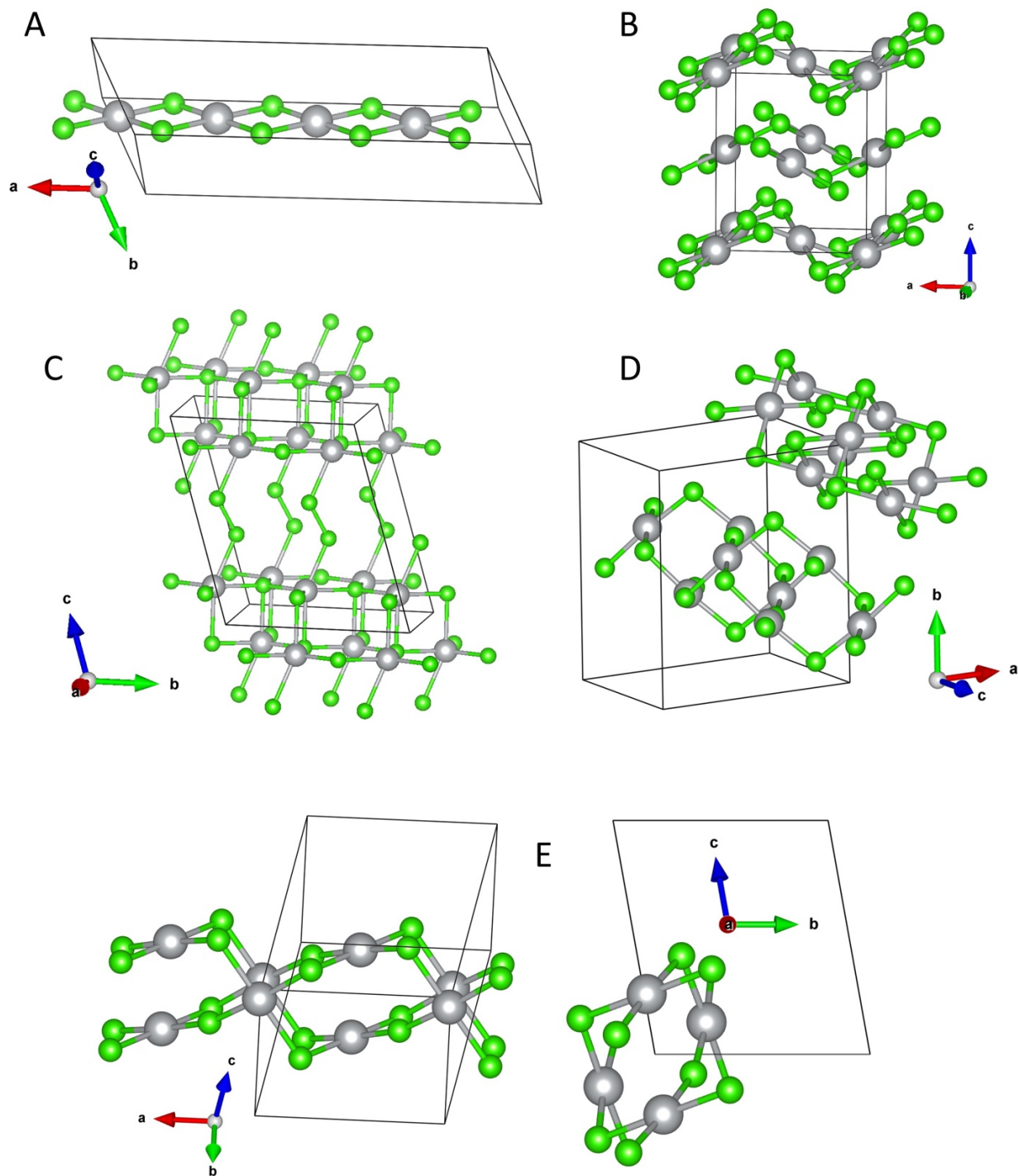
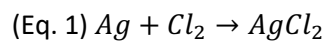
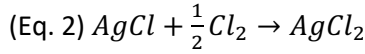


Fig. 1. Selected structures of AgCl_2 candidate polymorphs. A – CuCl_2 -type, B – AgF_2 -type, C – Ag(I)r , D – AgF_2 -HP-type, E – AuCl_2 -type. Ag – grey, Cl – green.

Stability of the studied candidate structures was evaluated using two parameters: (a) **enthalpy of formation** (labelled henceforth as ΔH_f), according to a reaction:



and (b) **stability towards decomposition** into AgCl and Cl₂ (ΔH_r), or more precisely, the enthalpy of reaction:



Defined in this manner, both parameters indicate thermodynamic instability when positive. Fig. 2 shows plots of stability of studied AgCl₂ candidate types in terms of ΔH_r for all three methods used in this work. Enthalpy of Ag + Cl₂ mixture relative to AgCl + ½Cl₂ is also plotted for comparison.

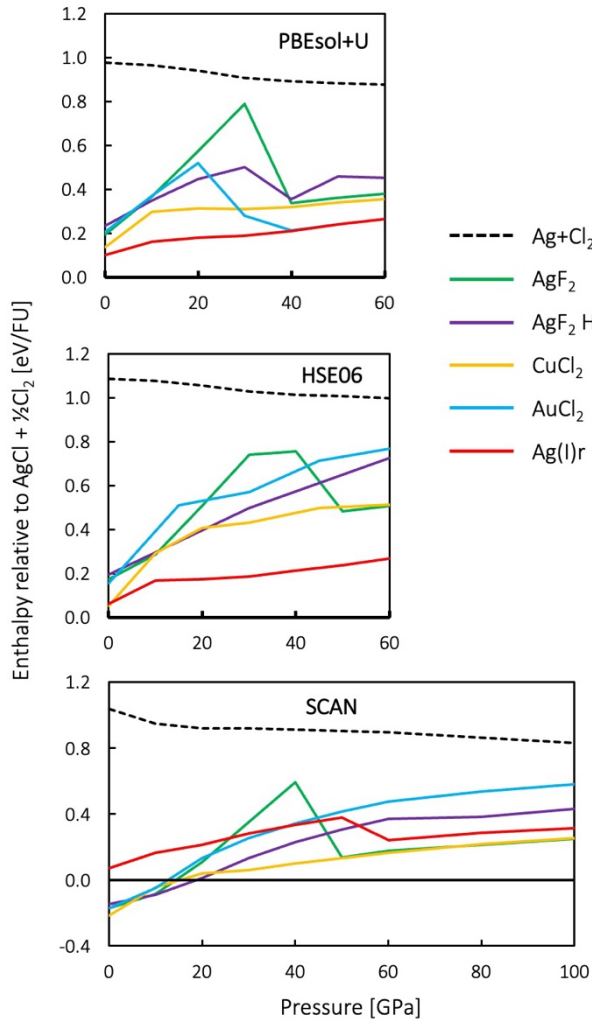


Fig. 2. Stability of selected studied polymorphs of AgCl₂, plotted as enthalpy per formula unit relative to AgCl + ½Cl₂ (ΔH_r). Top panel – PBEsol+U (GGA functional), middle panel – HSE06 (hybrid functional), bottom panel – SCAN (meta-GGA functional). FU – formula unit.

The studied polymorphs exhibit negative (favorable) enthalpies of formation within the entire studied pressure range in all three computational approaches. This is indirectly visible in fig. 2 as the fact that curves for those polymorphs lie below the curve for Ag + Cl₂. On the other hand, they were found to be unstable in terms of ΔH_r in the entire studied pressure range within PBEsol+U and HSE06. However, results of SCAN calculations indicate moderate stability of Ag^ICl₂ polymorphs below ca. 20 GPa. Ag(I)r polymorph is the most stable among AgCl₂ candidate structures, according to PBEsol+U and HSE06 results,

while this is not the case in SCAN picture. Given that it contains separate sub-phases of AgCl and Cl₂, this further points to an instability towards charge transfer and phase separation.

The initial set of calculations was performed within the PBEsol+U approach, as the least computationally demanding. It was found that the Ag(I)h type collapses upon compression to 10 GPa into the Ag(I)r structure and it was not considered any further in the analogous HSE06 and SCAN calculations. Similarly, MnO₂ type was also neglected past the PBEsol+U approach, as it was found to be the least stable in terms of ΔH_r among the studied types. Therefore, these two polymorphs are not taken into account in figures 1, 2 and 3.

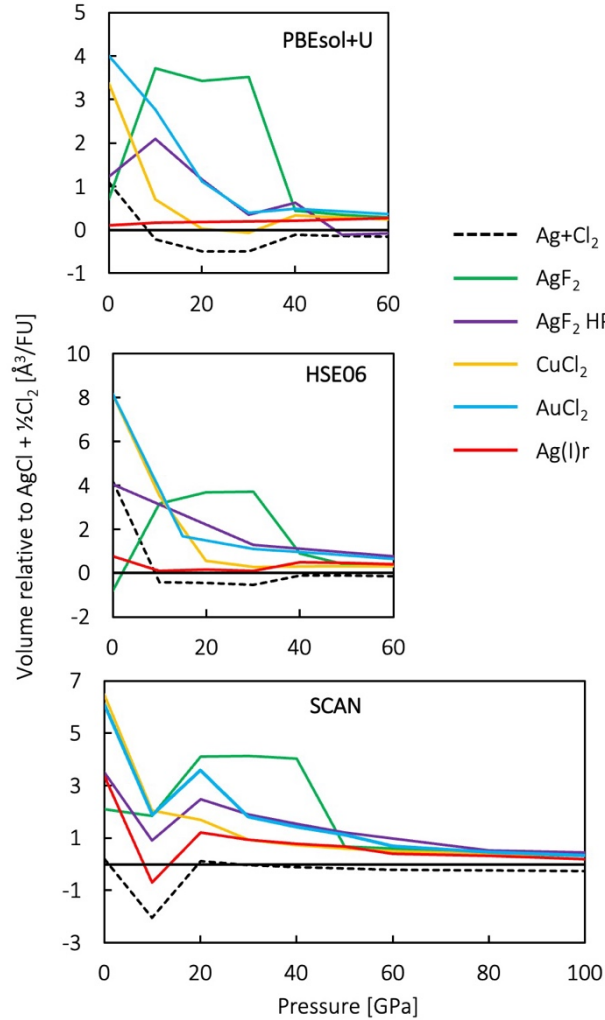


Fig. 3. Volume of selected studied polymorphs of AgCl₂ relative to AgCl + ½Cl₂. Top panel – PBEsol+U, middle panel – HSE06 (hybrid functional), bottom panel – SCAN (meta-GGA functional). FU – formula unit.

Fig. 3 compares relative volume (ΔV_r) of the studied polymorphs with respect to AgCl + ½Cl₂ mixture. Since the pV term becomes a considerable contribution to enthalpy at elevated pressures, the fact that most of the candidates for AgCl₂ considered here have a positive ΔV_r can be seen as an important factor leading to their relative instability. However, it should be noted that only HSE06 accurately reproduces ambient-pressure volumes of AgCl and Cl₂. PBEsol+U underestimates the volume of AgCl and Cl₂, while SCAN – that of Cl₂. Therefore, ΔV_r values at 0 GPa in fig. 3, and by extension – initial

compressibilities – should be taken with a grain of salt. A noticeable dip at 10 GPa within the SCAN approach is likely a manifestation of this. The computationally demanding HSE06 results are likely to be the most correct.

Some of the features in figures 2 and 3, such as abrupt changes of relative energies or volumes, and apparent convergence of plots corresponding to different polymorphs are indicative of structural transitions. The nature and implication of those transition will be discussed in the next section.

Pressure-induced structural transitions

As an introduction to analysis of structural transitions of AgCl_2 polymorphs, let us first discuss the Ag(I)r solution. As mentioned before, this structure is made up of subunits of rocksalt-type AgCl and of Cl_2 molecules. Within the studied pressure range, it undergoes structural rearrangements, which can be approximated as a sequence of deformations of the AgCl double layers, leading from a fundamentally NaCl-like coordination patterns to CsCl-like patterns, with increasing coordination number of Ag atoms. Importantly, it should be stressed again that this structure emerged as one of the lowest-energy solutions in an evolutionary algorithm structural search reported in the previous contribution. [6] It should not be treated as a viable candidate for the structure of AgCl_2 , but rather as a manifestation of the proclivity of the studied system towards charge transfer and phase separation. The case for instability of $\text{Ag}^{\text{II}}\text{Cl}_2$ towards these processes is further strengthened by the fact that the Ag(I)r polymorph remains the most stable (with respect to ΔH_f) throughout the studied pressure range in both PBEsol+U and HSE06 approaches. A noticeable drop in ΔH_f between 50 and 60 GPa for this polymorph in the SCAN approach was the reason for extending the studied pressure range to 100 GPa in this case. However, this drop is a result for NaCl-CsCl-like transition in the AgCl subphase, which is more abrupt than in analogous PBEsol+U and HSE06 calculations. No further phase transitions for Ag(I)r polymorph are observed up to 100 GPa.

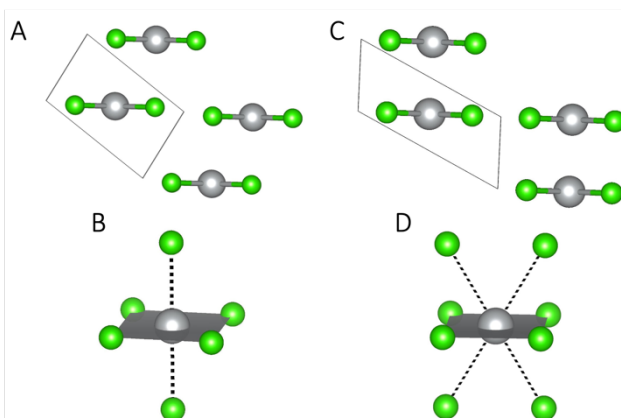


Fig. 4. Structural changes in CuCl_2 -polymorph. A and C – view along the direction of chain propagation at 10 and 20 GPa, respectively. B and D – view of local coordination of Ag at 10 and 20 GPa, respectively. Ag – grey, Cl – green.

The CuCl_2 -type polymorph emerges as the most structurally robust in this study, as it does not undergo any collapse or drastic deformation in the studied pressure range, maintaining a relatively low ΔV_f in all three methods. The only change to the structure of this polymorph occurs in terms of arrangement of chains relative to one another. Up to 10 GPa (in all three computational approaches), the chains are positioned as in fig. 4A, resulting in octahedral coordination of Ag atoms (fig. 4B). The octahedra are elongated by 29%, 29% and 25%, according to PBEsol, HSE06 and SCAN, respectively. By account of all three methods, the arrangement changes between 10 and 20 GPa, leading to a 4+4 coordination of Ag

atoms, with the 4 inter-chain contacts longer by 23 to 33%, depending on the method (fig. 4D). This is achieved in different ways: in PBEsol+U and HSE06 results, the chains move relative to one another in a direction perpendicular to direction of propagation (fig. 4C). In SCAN approach, this is achieved through a change of one of the unit cell angles, which results in sliding the chains relative to each other. The resulting 4+4 coordination is the same in all cases (fig. 4D), but the longer Cl contacts are aligned parallel (in SCAN) or perpendicular (in PBEsol+U and HSE06) to direction of propagation. Further compression to 30 GPa transforms the structure into that seen at 20 GPa in PBEsol+U and HSE06 pictures. All of these transitions can be seen as a means to achieve a more efficient packing of chains (as evidenced by increasing coordination number of Ag). Changes in local coordination of Ag atoms in this polymorph are plotted in the top panel of fig. 6.

Another result of these rearrangements is a reduction of Cl...Cl distances between neighboring chains. These distances drop from ca. 3.8 to 2.7 Å between 0 and 60 GPa in HSE06, compared to 3.2 to 2.5 Å in PBEsol+U and 3.5 to 2.8 Å in SCAN. Recall that only HSE06 correctly reproduced the ambient pressure (low-temperature) volume of solid molecular Cl₂ at 0 GPa, so these results further testify to the superiority of HSE06 in describing weak interactions compared to the other two methods utilized here (and free from the explicit van der Waals terms). Importantly, all of these distances are larger than the Cl-Cl bond in solid molecular Cl₂, which remains at ca. 2.00 Å and contracts very little (less than 0.05 Å) with compression in results from all three methods. Additionally, this polymorph was further optimized at 100 GPa with PBEsol+U and SCAN methods and does not undergo any structural modifications in that pressure range.

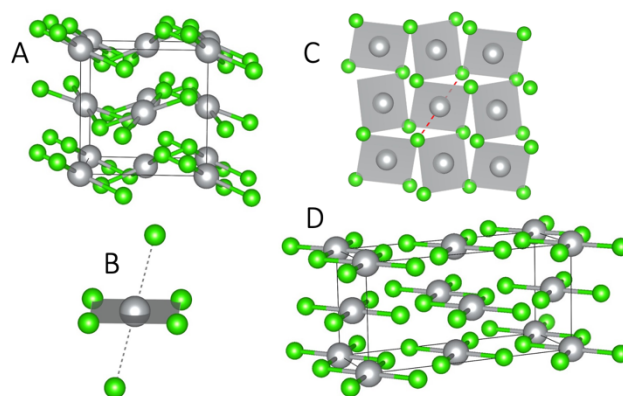


Fig. 5. Structural features of AgF₂-type polymorph: A – ambient-pressure structure; B – local coordination of Ag in the ambient-pressure structure; C – one layer at 40 GPa in HSE06 approach. Note that axial Cl atoms are now within the same layer, a pair of those contacts is marked with red dashed line; D – structure resulting from phase transition between 40 and 50 GPa (30 and 40 GPa in PBEsol+U approach). Note the CuCl₂-like chains. Ag – grey, Cl – green.

AgF₂-type polymorph undergoes substantial structural rearrangements with increasing pressure. At 0 GPa, it adopts a layered structure (fig. 5A), in which every Ag atom forms 4 in-layer bonds with Cl atoms, with two additional Cl atoms from adjacent layers together constituting a distorted octahedral coordination (fig. 5B). The axial Cl contacts are noticeably longer (by 23%, 33% and 27% in PBEsol+U, HSE06 and SCAN, respectively) than equatorial ones. The same phenomenon is observed in AgF₂ and in general, elongated octahedral coordination is a well-documented phenomenon in silver(II) fluorides (which includes ternary compounds). [10] This is usually attributed to Jahn-Teller effect, whereby a vibronic instability leads to elongation or contraction of bonds along one of the three axes of octahedron, which

lowers the overall electronic energy. Upon compression, this elongation is reduced in AgCl_2 down to 1%-2% at 30 GPa in both PBEsol+U and SCAN results. Further increase of pressure (40 GPa in PBEsol+U and 50 GPa in SCAN) leads to a structural transition into a polymorph consisting of 1D chains similar to those found in CuCl_2 -type polymorph (fig. 5D). In the HSE06 picture, the contraction is less pronounced – down to 10% at 30 GPa, and the transition to the chain polymorph occurs via a different layered structure observed at 40 GPa, where the layers become more corrugated and more separated from each other (fig. 5C). Ag atoms retain an approximately octahedral coordination, but the axial Cl contacts are now within the same layer as $[\text{AgCl}_4]$ squares. The elongation of octahedra due to Jahn-Teller effect is still noticeable (9%). Further compression to 50 GPa leads to a collapse to chains as in the other two methods. Changes in local coordination of Ag atoms in this polymorph are plotted in the bottom panel of fig. 6.

The transitions described above can be seen as an abrupt drop in relative enthalpy in fig. 2. In the previous contribution discussing relative stability of AgCl_2 candidate structures, AgF_2 -type emerged as the most likely candidate at higher pressures due to its comparatively low molar volume among the considered structures. [6] However, it appears that compression of AgF_2 -type produces a lot of strain in the structure, as evidenced by a strong increase of ΔH_r (fig. 2), which is released through the aforementioned transition.

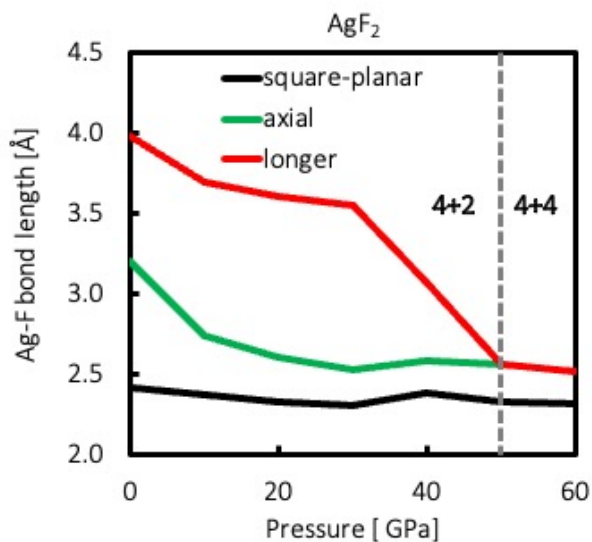
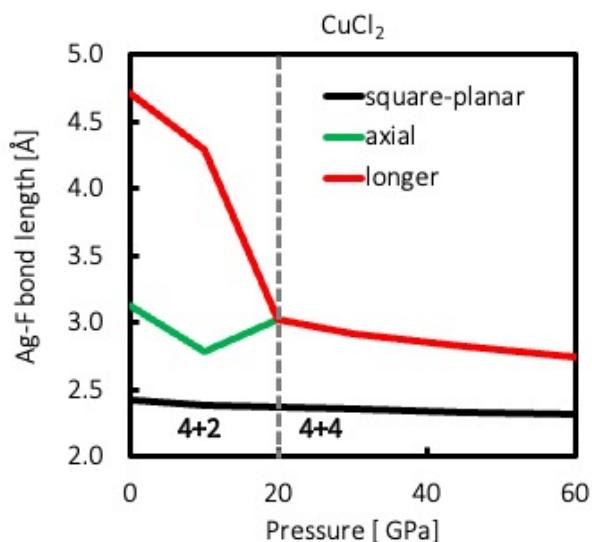


Fig. 6. Pressure dependence of Ag-F distances in CuCl_2 -type and AgF_2 -type polymorphs in the HSE06 picture.

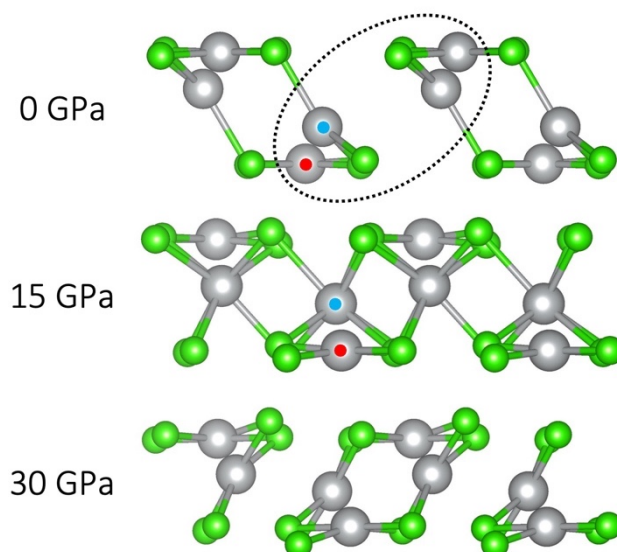


Fig. 7. Structural transition of AuCl_2 -type polymorph in the HSE06 picture. Nanotubes are viewed along the axis of propagation. Blue and red circles indicate Ag(I) and Ag(III) species, respectively.

Arguably the most interesting pattern of pressure-induced transitions can be observed in the AuCl_2 -type nanotubular polymorph. The differences in outcomes of compression between the three computational approaches are the most pronounced for this system, although upon closer look we can identify their fundamental similarity. Recall that in the HSE06 approach, AuCl_2 -type is mixed-valent: Ag(I) species are connected to 3 Cl atoms in an approximately flat triangular pattern, while the Ag(III) sites appear as $[\text{AgCl}_4]$ square units, which are analogous to those in AgF_3 . [11] At 0 GPa, the triangular contacts average 2.53 Å, while the bonds in square units are 2.29 Å, which is even shorter than for Ag(II) in $[\text{AgCl}_4]$ square in CuCl_2 -type and AgF_2 -type polymorphs at the same pressure. This supports the assignment of the sites as Ag(I) and as Ag(III), respectively. Compression to 15 GPa induces a change in local coordination of the Ag(I) species, which picks up 4 Cl atoms along the axis perpendicular to the plane of the former triangle, resulting in a 4+3 coordination, with an average bond length of 2.61 Å. Meanwhile, the Ag(III) subunit retains a square coordination with a shorter average bond length of 2.27 Å. Further compression to 30 GPa leads to a rearrangement of nanotubes, which are now formed by a different combination of Ag and Cl atoms; importantly, all Ag atoms are coordinated by 4 Cl atoms in an approximately square-planar manner, with an average for the formerly Ag(III) sites at 2.33 Å and the formerly Ag(I) ones – 2.38 Å. This convergence of the two sites in terms of local coordination points to a comproportionation process, whereby all Ag sites are now nominally Ag(II) species. The transition described above is shown in fig. 7.

A very different scenario is observed in the SCAN picture (fig. 8). At 0 GPa, the two Ag sites are already equivalent, but upon compression to 10 GPa, the local square-planar coordination of one of them is rotated by 90 degrees i.e., two of its four nearest Cl neighbors are substituted for another two, which leads to connections between nanotubes in the c direction. Further compression to 30 GPa results in an inward contraction of individual nanotubes. The local coordination of the Ag sites marked with red circle changes to more uniformly octahedral – a fifth Cl atom is picked up from a neighboring nanotube along the axis perpendicular to the $[\text{AgCl}_4]$ plane. The average length of the five Ag–Cl bonds for this Ag site is 2.51 Å

(2.45-2.55 Å). The sixth nearest neighbor, on the opposite side of the former $[\text{AgCl}_4]$ is actually another Ag atom, located at a distance of 2.70 Å. (This connection is marked with a dashed line in fig. 8.) Importantly, this new Ag...Ag contact is consistently shorter than the Ag–Ag distance in metallic silver at corresponding pressures (from SCAN calculations): 2.70 Å vs. 2.72 Å (30 GPa), 2.64 Å vs. 2.69 Å (40 GPa) and 2.60 Å vs. 2.67 Å (50 GPa). This leads us to infer a formation of a weak Ag-Ag interaction in this polymorph, which is a very interesting finding and reminiscent of a recent work, where a silver subchloride Ag_8Cl_6 was predicted, featuring $[\text{Ag}_6]$ subunits within its structure. [12] Further compression above 50 GPa leads to a substantial structural rearrangement: AgCl-like chains with square cross-section are formed, interspersed with Cl_2 molecules.

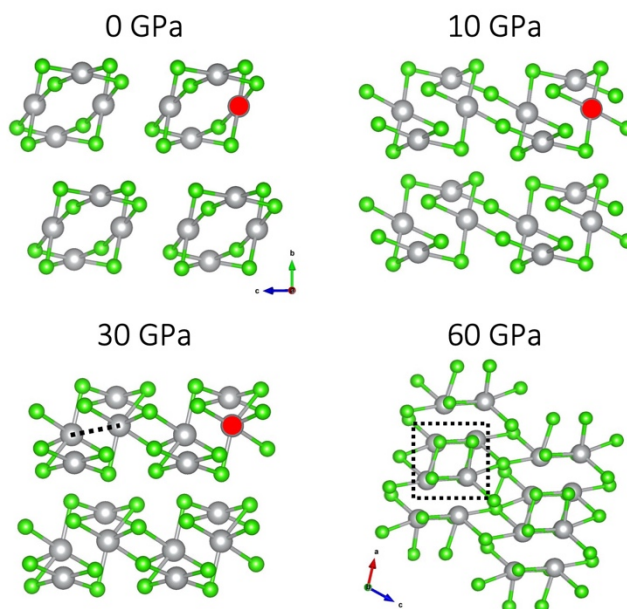


Fig. 8. Structural transition of AuCl_2 -type polymorph in the SCAN picture. Nanotubes are viewed along the axis of propagation from 0 to 30 GPa. Note a different projection at 60 GPa, along the newly formed $[\text{AgCl}]$ square nanowires. Red circles mark the Ag atom which experiences the pronounced changes in local coordination in the 0-30 GPa range.

A similar picture emerges from the PBEsol+U approach. As in SCAN results, compression to 10 GPa leads to a rearrangement of local coordination of half of Ag sites. The subsequent contraction of nanotubes and formation of short Ag...Ag contacts is observed at a lower pressure of 20 GPa (compared to 30 GPa in SCAN). Upon further pressure increase to 30 GPa, a structure similar to Ag(I)r polymorph is formed, consisting of double layers of rocksalt-like AgCl interspersed with Cl atoms. The difference is that here, no discernible Cl-Cl molecules are formed – the distance between Cl atoms lying between AgCl layers is ca. 2.3 Å, compared to ca. 2.0 Å in solid molecular Cl_2 and in Ag(I)r polymorph. This is likely an artificial result, which will be further discussed in the “Electronic structure” section. Finally, compression to 40 GPa leads to rearrangement within AgCl layers, which increases the coordination number of Ag from 6 to 7 and the coordination environment resembles that in CsCl. Cl_2 molecules between the AgCl layers, characteristic of Ag(I)r polymorph, can also be discerned. Indeed, as can be seen in fig. 2, this solution also converges with Ag(I)r polymorph in terms of ΔH_r .

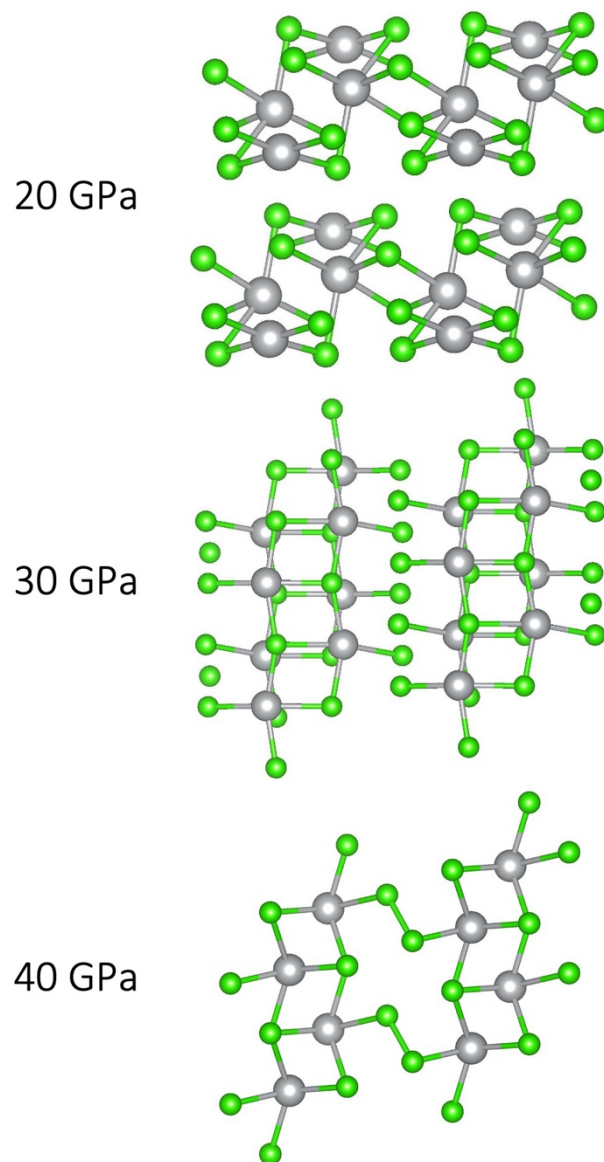


Fig. 9. Structural transitions of AuCl₂-type polymorph in the PBEsol+U picture.

As in the case of Ag(I)r solutions, formation of separate domains of AgCl and Cl₂ during structural transitions of AuCl₂-type in PBEsol+U and SCAN picture, can be interpreted as another manifestation of the system's tendency for AgCl + ½Cl₂ phase separation, rather than as viable structural candidates. However, it should be pointed out that sodium and potassium chlorides with exotic stoichiometries as e.g. NaCl or Na₃Cl, have been predicted in the past. [13,14]

Nanotubular AgF₂-HP-type polymorph undergoes a structural collapse above 30 GPa in PBEsol+U results and above 60 GPa in SCAN results. The final structures do not resemble any of those discussed above; rather, they feature domains of connections between Ag and Cl atoms which do not form any extended and discernible pattern, and are instead interspersed with Cl₂ molecules. Since those solutions are consistently very high in relative enthalpy (ΔH_r), they will not be further analyzed here.

Electronic properties

As inferred from the previous paper, [6] antiferromagnetic superexchange in $\text{Ag}^{\text{II}}\text{Cl}_2$ can, in principle, be expected to be strong, since Ag–Cl bonding in this hypothetical compound would likely be more covalent in nature than in its AgF_2 counterpart. Of course, AgCl – the only currently known binary combination of silver and chlorine – is an ionic solid, as is AgF . However, previous studies of AgF_2 demonstrated a covalent character of Ag–F bonding in that compound, evidenced by X-ray photoelectron spectroscopy [15] and by optical spectra. [16] In the former study, covalency increased in the sequence $\text{AgF} \rightarrow \text{AgF}_2 \rightarrow \text{AgF}_3$. Therefore, it is reasonable to expect a similar trend in AgCl_x compounds. On the other hand, Cl^- anions are larger and more diffuse and are therefore softer Lewis bases than F^- anions, which makes them more vulnerable to the strongly oxidizing properties of $\text{Ag}(\text{II})$ cations. In addition, increasing pressure and the consequent reduction of interatomic distances increases orbital overlap, leading to broadening of electronic bands, which ultimately results in metallization of most known compounds (both ionic and covalent). [7]

Electronic properties of the studied AgCl_2 candidate polymorphs were scrutinized in terms of (a) magnetic moments on Ag atoms and (b) fundamental band gap at the Fermi level in electronic density of states (eDOS) graphs. As it turns out, changes in the two parameters are strongly correlated in that the pressure at which the band gap closes coincides with disappearance of magnetic moment on Ag atoms.

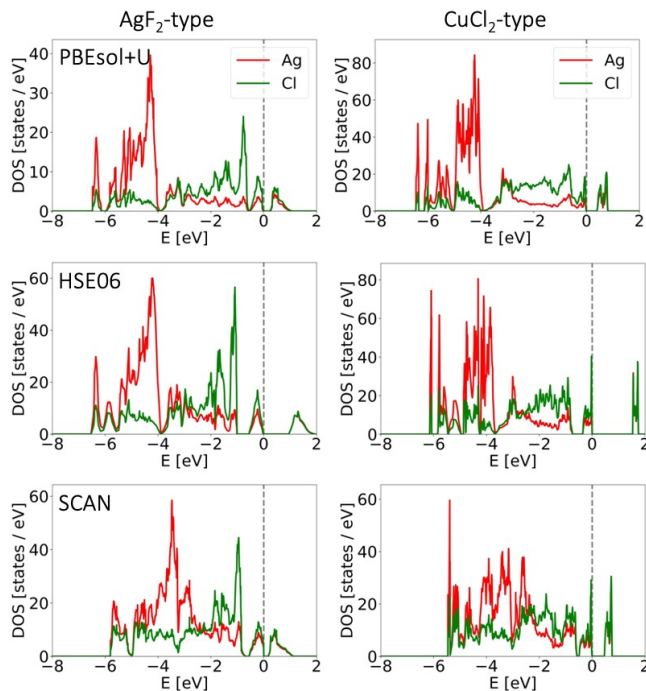


Fig. 10. Comparison of eDOS plots for AgF_2 -type and CuCl_2 -type between different computational methods at 0 GPa.

An example of eDOS plots – for AgF_2 -type and CuCl_2 -type – at 0 GPa and comparison between the three computational methods is presented in fig. 10. One noticeable feature is the composition of conduction band. In principle, AgCl_2 , just like the known AgF_2 , is expected to be a charge-transfer insulator, where the band gap arises between filled nonmetal states and empty metal states (upper Hubbard band, UHB). [17] While this is certainly the case in AgCl_2 , we can see a substantial admixing of Cl states to the

conduction band, with an almost perfect overlap and approximately equal contributions from Ag and Cl states. This indicates a strong covalence of the Ag–Cl bonds that is comparable or indeed even stronger than in AgF₂. [15] It should also be pointed out that “insulator” in this case refers to a non-zero band gap resulting from electronic correlation as per the aforementioned Zaanen-Sawatzky-Allen model. [17] Clearly, with a band gap in the range 0.2-1.5 eV (depending on the method) (fig. 10), the two AgCl₂ polymorphs in question can be more accurately described as semiconductors.

Table 1 compares metallization pressure for selected polymorphs and between three methods. Metallization pressure is defined here as the lowest pressure point at which a solution exhibits null magnetic moments and null band gap. It can be seen that this value is the highest in HSE06 results. This coincides with the observation that the band gap is the largest for AgF₂-type and CuCl₂-type polymorphs in the HSE06 picture (fig. 10). The differences between methods likely stem from the inclusion of exchange correlation in the hybrid-DFT-type functional, while in GGA-type PBEsol+U approach, electronic correlation, which is crucial for modelling open-subshell systems such as Ag(II) compounds, is only taken into account through *U* and *J* parameters (mentioned in “Methods” section). HSE06 results can likely be considered the most accurate in the case of this system.

Table 1. Pressure of metallization for different polymorphs of AgCl₂.

	<u>PBEsol+U</u>	<u>HSE06</u>	<u>SCAN</u>
AgF ₂ -type	20 GPa	>60 GPa*	10 GPa
CuCl ₂ -type	10 GPa	45 GPa	10 GPa
AgF ₂ HP-type	0 GPa	60 GPa	10 GPa
AuCl ₂ -type†	0 GPa	15 GPa‡	10 GPa

Footnotes: *Although transformed into chains similar to CuCl₂-type, the polymorph retains residual magnetic moment and non-zero band gap at the maximal studied pressure of 60 GPa. Magnetic coupling is FM intra-chain and AFM inter-chain; †Reopening of band gap occurs at higher pressures – see text. ‡This polymorph is mixed-valent in HSE06 picture and is non-magnetic at 0 GPa.

The phase-separated Ag(I)r polymorph remains insulating within the studied pressure range and by account of all three methods. Structural transitions into phase-separated solutions observed for AuCl₂-type polymorph, which were discussed in the previous section, are also associated with reopening of the band gap. That is because constituent parts of these solutions – sublattices made up of ionic AgCl and of molecular Cl₂ – are insulators. The fact that the solution for AuCl₂-type polymorph at 30 GPa in PBEsol+U picture retains metallic character after the aforementioned transition stems from the presence of dangling, unpaired Cl atoms on the outside of AgCl layers. Such arrangement should be unstable towards a Peierls distortion and formation of Cl₂ molecules, which is indeed what happens upon further compression to 40 GPa, and in SCAN picture. This testifies to the relatively poor suitability of PBEsol+U for describing electronic correlation.

Discussion

The results presented above shed some light on properties and prospects of synthesis of the hypothetical AgCl₂. Structural transitions of CuCl₂ and AgF₂ types reveal the tendency of the system to avoid repulsion between axial Cl atoms and filled d(z²) orbital of Ag atoms – through relative displacement of chains in the former and through transition from a layered 2D structure into 1D chains in the latter. A similar tendency is seen in pressure-induced phase transitions of AgF₂, where the high-pressure

nanotubular structure can be viewed as a means both to maximize coordination number and to minimize the repulsion from the Ag $d(z^2)$ lone pair. [4] The transitions of AuCl_2 -type and the relative stability of Ag(I)r polymorph firmly indicate that $\text{Ag}^{\text{II}}\text{Cl}_2$ is unstable towards charge transfer and phase separation into AgCl and Cl_2 .

It is important to note that the overall picture which emerges from data presented here is remarkably consistent across the three computational methods employed: GGA DFT (PBEsol+U), hybrid-DFT (HSE06) and meta-GGA DFT (SCAN). The observed structural and electronic changes are essentially the same between the three computational methods, differing only in terms of pressure at which they occur. Fundamentally, phase transitions observed in the studied polymorphs unfold upon pressure-induced decrease in distance between 1D or 2D structural constituents (chains, nanotubes, layers), which entails overcoming weak repulsive interactions between them, and the HSE06 functional, among the three methods utilized here, is best suited for description of those interactions. In particular, this work shows that the prediction of stability of AgF_2 -type polymorph, which was based on a reasonable extrapolation from ambient-pressure data, nevertheless turned out not to be false. [6]

Of course, this work does not exhaust the list of possible candidates for the structure of AgCl_2 . Although the studied candidates generally retain a positive enthalpy with respect to decomposition into $\text{AgCl} + \frac{1}{2}\text{Cl}_2$, it is worth noting that the CuCl_2 -type chain structure does not collapse into phase-separated polymorph even at 100 GPa in PBEsol+U and SCAN results. Analogous HSE06 calculations at 100 GPa were not performed, but based on the observation made here that transition pressures are reliably the highest within HSE06 approach, it is reasonable to predict that such collapse would not be seen in HSE06 picture at 100 GPa, either. The apparent lack of such transition pathway could mean that, in principle, obtaining it as a metastable phase could be possible if e.g., elevated temperatures are used together with moderate pressures. Our previous results [6], as well as earlier predictions by other authors [18,19], all consistently suggest that $\text{Ag}^{\text{II}}\text{Cl}_2$, if ever obtained, would likely be metastable.

Although the current study was focused on AgCl_2 stoichiometry only, the results of this study permit us to extrapolate observed trends towards the AgCl_3 . The tendency of AgCl_2 stoichiometry to undergo decomposition to $(\text{AgCl})(\text{Cl}_2)_{\frac{1}{2}}$ may suggest that even at larger Cl contents, i.e. for AgCl_3 stoichiometry, one will observe phase separation to $(\text{AgCl})(\text{Cl}_2)$, or $\text{Ag}^+(\text{Cl}_3^-)$. [20] A similar result is indicated by theoretical study for isolated AgCl_3 molecules in the gas phase. [21]

Methods

Calculations were carried out using VASP software. [22–26] Overall, three different computational methods were utilized (underlined are the names by which they are referred to throughout this work):

- I. PBEsol+U approach. GGA-type Perdew-Burke-Ernzerhof functional adapted for solids (PBEsol) [27] was used, additionally taking into account Coulombic interactions between d electrons through U and J parameters [28] explicitly set to 5 eV and 1 eV, respectively, and with correction for van der Waals interactions. [29] Plane-wave cutoff energy was set to 800 eV and k-space sampling of $\text{ca. } 2\pi \times 0.04 \text{ \AA}^{-1}$ was used, with self-consistent-field convergence criterion of 10^{-7} eV. A denser k-spacing of $\text{ca. } 2\pi \times 0.03 \text{ \AA}^{-1}$ was used for electronic density of states (eDOS) calculations.
- II. HSE06 approach. Hybrid-DFT HSE06 functional was utilized. [30] Due to higher computational load of this method, a coarser k-space sampling of $\text{ca. } 2\pi \times 0.04 \text{ \AA}^{-1}$ was used and plane-wave cut-off was set to 520 eV, with self-consistent-field convergence criterion of 10^{-7} eV.

- III. SCAN approach. Meta-GGA-type, strongly constrained and appropriately normed (SCAN) functional was used, [31] with correction for van der Waals interactions. [32] Plane-wave cut-off energy was set to 800 eV and k-space sampling of ca. $2\pi \times 0.035 \text{ \AA}^{-1}$ was used, with self-consistent-field convergence criterion of 5×10^{-7} eV. A denser k-spacing of ca. $2\pi \times 0.025 \text{ \AA}^{-1}$ was used for eDOS calculations.

The studied pressure range was 0 to 60 gigapascals (GPa), additionally extended to 100 GPa for SCAN calculations. Pressure step was 10 GPa up to 60 GPa (or in some cases 15 GPa in HSE06 approach) and 20 GPa above 60 GPa. Cl_2 was considered in its solid polymorph with *Cmca* space group, which is known to be stable in the entire pressure range considered here. [33] Similarly, metallic silver is also stable in its fcc structure in that range. [34] Known phase transitions of AgCl were taken into account when calculating relative enthalpy of AgCl_2 polymorphs. [35] A primitive unit cell of the KOH-type, high-pressure polymorph of AgCl was utilized in calculations, since it can be used to accurately describe the continuous nature of NaCl-KOH-TlI-CsCl sequence of phase transitions of AgCl. [35,36]

References

1. Grochala, W. Silverland: the Realm of Compounds of Divalent Silver—and Why They are Interesting. *Journal of Superconductivity and Novel Magnetism* **31**, 737–752 (2018).
2. Gawraczyński, J. *et al.* Silver route to cuprate analogs. *Proceedings of the National Academy of Sciences* **116**, 1495–1500 (2019).
3. Grzelak, A. *et al.* Metal fluoride nanotubes featuring square-planar building blocks in a high-pressure polymorph of AgF_2 . *Dalton Transactions* **46**, 14742–14745 (2017).
4. Grzelak, A. *et al.* High-Pressure Behavior of Silver Fluorides up to 40 GPa. *Inorganic Chemistry* **56**, 14651–14661 (2017).
5. Kurzydłowski, D., Derzsi, M., Zurek, E. & Grochala, W. Fluorides of Silver Under Large Compression. *Chemistry – A European Journal* **27**, (2021).
6. Derzsi, M., Grzelak, A., Kondratiuk, P., Tokár, K. & Grochala, W. Quest for Compounds at the Verge of Charge Transfer Instabilities: The Case of Silver(II) Chloride. *Crystals* **9**, 423 (2019).
7. Grochala, W., Hoffmann, R., Feng, J. & Ashcroft, N. W. The chemical imagination at work in very tight places. *Angewandte Chemie - International Edition* **46**, 3620–3642 (2007).
8. Banks, M. G. *et al.* Magnetic ordering in the frustrated Heisenberg chain system cupric chloride CuCl_2 . *Physical Review B* **80**, (2009).
9. Dell’Amico, D. B., Calderazzo, F., Marchetti, F. & Merlino, S. Synthesis and molecular structure of $[\text{Au}_4\text{Cl}_8]$, and the isolation of $[\text{Pt}(\text{CO})\text{Cl}_5]^-$ in thionyl chloride. *Journal of the Chemical Society, Dalton Transactions* **1982**, 2257 (1982).
10. Kurzydłowski, D. *et al.* Local and Cooperative Jahn-Teller Effect and Resultant Magnetic Properties of M_2AgF_4 ($\text{M} = \text{Na-Cs}$) Phases. *Inorganic Chemistry* **55**, 11479–11489 (2016).

11. Žemva, B. *et al.* Silver Trifluoride: Preparation, Crystal Structure, Some Properties, and Comparison with AuF₃. *Journal of the American Chemical Society* **113**, 4192–4198 (1991).
12. Uhliar, M. & Derzsi, M. Clustered silver subchloride - in preparation. (2021).
13. Zhang, W. *et al.* Stability of numerous novel potassium chlorides at high pressure. *Scientific Reports* **6**, 26265 (2016).
14. Zhang, W. *et al.* Unexpected Stable Stoichiometries of Sodium Chlorides. *Science* **342**, 1502–1505 (2013).
15. Grochala, W., Egdell, R. G., Edwards, P. P., Mazej, Z. & Žemva, B. On the covalency of silver-fluorine bonds in compounds of silver(I), silver(II) and silver(III). *ChemPhysChem* **4**, 997–1001 (2003).
16. Bachar, N. *et al.* Charge Transfer and dd excitations in AgF₂. *arXiv preprint arXiv:2105.08862* (2021).
17. Zaanen, J., Sawatzky, G. A. & Allen, J. W. Band gaps and electronic structure of transition-metal compounds. *Physical Review Letters* **55**, 418–421 (1985).
18. Morris, D. F. C. The instability of some dihalides of copper and silver. *Journal of Physics and Chemistry of Solids* **7**, 214–217 (1958).
19. Rossini, F. D., Wagman, D. D., Evans, W. H., Levine, S. & Jaffe, I. Selected values of chemical thermodynamic properties. *Circular of the Bureau of Standards* **500**, (1952).
20. Haller, H. & Riedel, S. Recent discoveries of polyhalogen anions - From bromine to fluorine. *Zeitschrift für Anorganische und Allgemeine Chemie* **640**, 1281–1291 (2014).
21. Müller-Rösing, H. C., Schulz, A. & Hargittai, M. Structure and bonding in silver halides. A quantum chemical study of the monomers: Ag₂X, AgX, AgX₂, and AgX₃ (X = F, Cl, Br, I). *Journal of the American Chemical Society* **127**, 8133–8145 (2005).
22. Kresse, G. & Hafner, J. Ab initio molecular dynamics for liquid metals. *Physical Review B* **47**, 558–561 (1993).
23. Kresse, G. & Hafner, J. Ab initio molecular-dynamics simulation of the liquid-metalamorphous- semiconductor transition in germanium. *Physical Review B* **49**, 14251–14269 (1994).
24. Kresse, G. & Furthmüller, J. Efficiency of ab-initio total energy calculations for metals and semiconductors using a plane-wave basis set. *Computational Materials Science* **6**, 15–50 (1996).
25. Kresse, G. & Furthmüller, J. Efficient iterative schemes for ab initio total-energy calculations using a plane-wave basis set. *Physical Review B - Condensed Matter and Materials Physics* **54**, 11169–11186 (1996).
26. Kresse, G. & Joubert, D. From ultrasoft pseudopotentials to the projector augmented-wave method. *Physical Review B* **59**, 1758–1775 (1999).

27. Perdew, J. *et al.* Restoring the Density-Gradient Expansion for Exchange in Solids and Surfaces. *Physical Review Letters* **100**, 136406 (2008).
28. Liechtenstein, A. I., Anisimov, V. I. & Zaanen, J. Density-functional theory and strong interactions: Orbital ordering in Mott-Hubbard insulators. *Physical Review B* **52**, R5467–R5470 (1995).
29. Grimme, S., Antony, J., Ehrlich, S. & Krieg, H. A consistent and accurate *ab initio* parametrization of density functional dispersion correction (DFT-D) for the 94 elements H–Pu. *The Journal of Chemical Physics* **132**, (2010).
30. Krukau, A. v., Vydrov, O. A., Izmaylov, A. F. & Scuseria, G. E. Influence of the exchange screening parameter on the performance of screened hybrid functionals. *The Journal of Chemical Physics* **125**, 224106 (2006).
31. Sun, J., Ruzsinszky, A. & Perdew, J. P. Strongly Constrained and Appropriately Normed Semilocal Density Functional. *Physical Review Letters* **115**, 036402 (2015).
32. Peng, H., Yang, Z.-H., Perdew, J. P. & Sun, J. Versatile van der Waals Density Functional Based on a Meta-Generalized Gradient Approximation. *Physical Review X* **6**, 041005 (2016).
33. Dalladay-Simpson, P. *et al.* Band gap closure, incommensurability and molecular dissociation of dense chlorine. *Nature Communications* **10**, 1134 (2019).
34. Dewaele, A., Torrent, M., Loubeyre, P. & Mezouar, M. Compression curves of transition metals in the Mbar range: Experiments and projector augmented-wave calculations. *Physical Review B* **78**, 104102 (2008).
35. Hull, S. & Keen, D. Pressure-induced phase transitions in AgCl, AgBr, and AgI. *Physical Review B* **59**, 750–761 (1999).
36. Catti, M. & di Piazza, L. Phase equilibria and transition mechanisms in high-pressure AgCl by Ab initio methods. *Journal of Physical Chemistry B* **110**, 1576–1580 (2006).

Acknowledgments

A.G. would like to thank Dr. Mariana Derzsi for fruitful discussions and comments at the initial stage of this work's development. A.G. acknowledges the contribution from the Polish National Science Center (NCN) – Preludium project no. 2017/25/N/ST5/01976. This research was carried out with the support of the ICM computer center, University of Warsaw under grant SAPPHIRE (no. GA83-34 and G85-892).

Author contributions statement

A.G. and W.G. conceived the study. A.G. performed computations, analyzed the results, made the figures and wrote the manuscript. W.G. reviewed the manuscript.